

Density functional theory study of effect of NO annealing on electronic structures and carrier scattering properties of 4H-SiC(0001)/SiO₂ interface

Nahoto Funaki, Kosei Sugiyama, Mitsuharu Uemoto, and Tomoya Ono

*Department of Electrical and Electronic Engineering, Graduate School of Engineering,
Kobe University, Nada, Kobe 657-8501, Japan*

(Dated: 1 July 2025)

The effect of the nitrated layer introduced by NO annealing on the electronic structure and carrier scattering property of the 4H-SiC(0001)/SiO₂ interface is investigated by the density functional theory calculation using the interface models where the areal N atom density corresponds to that in practical devices. The areal N atom density is one third of the areal C atom density in practical devices. It is found that the nitrated layer screens the unfavorable Coulomb interaction of O atoms in the SiO₂. However, the electrons flowing under the nitrated layer are significantly scattered by the fluctuation of potential due to the low areal N atom density. These results imply that the areal N atom density should be increased so that the fluctuation of potential is suppressed.

SiC is a suitable material for future power electronics devices with high breakdown field, high carrier velocity, and a native oxide of SiO₂, making it ideal for metal-oxide-semiconductor field-effect transistors (MOSFETs). Among hundreds of polymorphs of SiC (e.g., 3C, 4H, and 6H), the most interesting commercially available polymorph is 4H-SiC, which can be grown as single-polymorph wafers.¹⁻⁴ However, the high channel resistance of SiC-MOSFETs limits their performance.^{5,6} This high resistance is expected to be attributed to the low field-effect mobility in SiC-MOSFETs, which is much lower than the ideal electron mobility ($\sim 1000 \text{ cm}^2\text{V}^{-1}\text{s}^{-1}$).⁷ By post-oxidation annealing with nitric oxide (NO),^{8,9} the maximum field-effect mobility, which is proportional to the product of Hall mobility and mobile carrier density, increases from 1–7 $\text{cm}^2\text{V}^{-1}\text{s}^{-1}$ ¹⁰ to 25–40 $\text{cm}^2\text{V}^{-1}\text{s}^{-1}$ for a 4H-SiC(0001) MOSFET.¹¹⁻¹³ Hatakeyama *et al.* reported that the Hall mobility is not improved by NO annealing while the mobile carrier density increases and the improvement in the field-effect mobility is due to the increase in the mobile carrier density.¹⁴ However, the impact of the nitrated layers introduced by NO annealing on the low Hall mobility and the increase of mobile carrier density is not fully clear.

Most SiC-MOSFETs are *n*-type, with electrons in the conduction band serving as carriers. The behavior of conduction band edge (CBE) states of a SiC bulk is like that of free electrons, which are so-called “floating states,”¹⁵ and sensitive to the local atomic structure at the interface.¹⁶ In practical devices, the 4H-SiC(0001) surface is not atomically flat, e.g., the 4H-SiC(0001) substrates possess atomic scale steps on their surfaces which are generated during the fabrication process.¹⁷ In our previous study, we have reported that the CBE states are affected by the Coulomb interaction of the O atoms in the SiO₂, which results in the discontinuity of the inversion layers at the step edge under gate bias.¹⁸ After NO annealing is carried out, the inserted nitrated layer screens the Coulomb interaction of the O atoms and the inversion layer becomes spatially continuous, resulting in the increase of the mobile carrier density. However, in the computational model for the interface after NO annealing in our previous study, the areal N atom density was the same as the areal C atom density and three times higher than that of practical devices.¹⁹ In this paper, the density functional theory (DFT)²⁰ calculation is carried out to investigate the effect of nitrated layers in which the areal N atom density is reduced so as to correspond to that in practical devices. It is found that the nitrated layer screens the Coulomb interaction even when the areal N atom density is reduced. However, the conducting electrons from the source to the drain are scattered by the fluctuation of potential due to the low areal N atom density, which implies that the interface with high areal N atom density is advantageous for electron conduction.

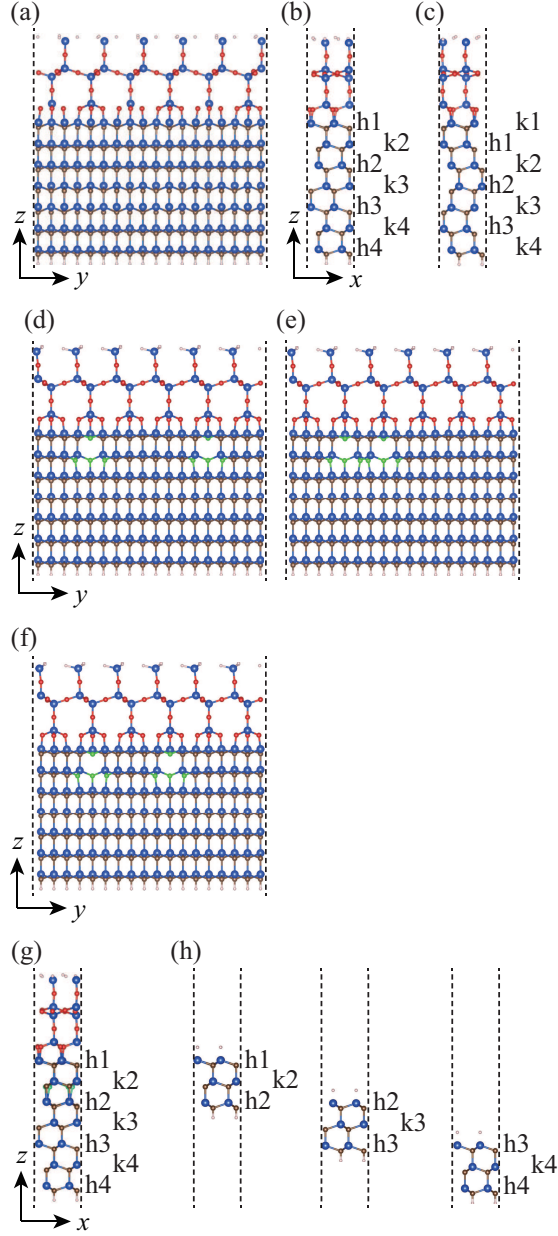


FIG. 1. Computational models for SiC/SiO₂ interface and SiC thin film. (a) Front view of the interface without any nitrated regions, (b) side view of the h-type interface without any nitrated regions, (c) side view of the k-type interface without any nitrated regions, (d)–(f) front view of the interface with nitrated regions, (g) side view of the h-type interface with nitrated regions, and (h) side views of thin films. (d)–(f) are labeled models 1, 2, and 3, respectively. Blue, red, brown, green, and gray balls are Si, O, C, N, and H atoms, respectively. Since the atomic structure of the k-type interface looks the same as that of the h-type interface when it is seen from the $[11\bar{2}0]$ direction, only the atomic structures of the h-type interfaces are shown for the front view.

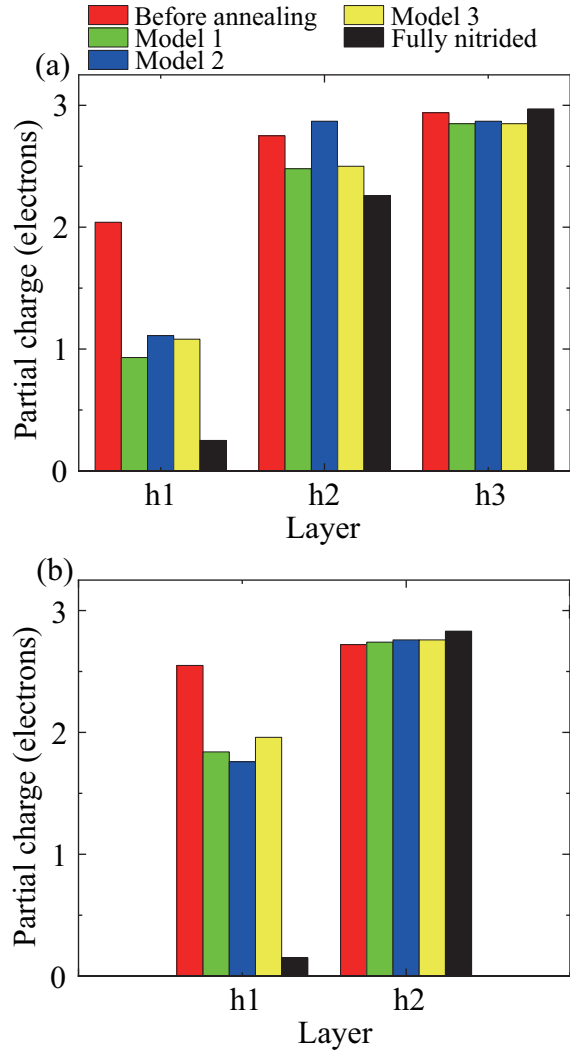


FIG. 2. Amount of partial charges of CBE states for (a) h- and (b) k-type interfaces in units of electrons.

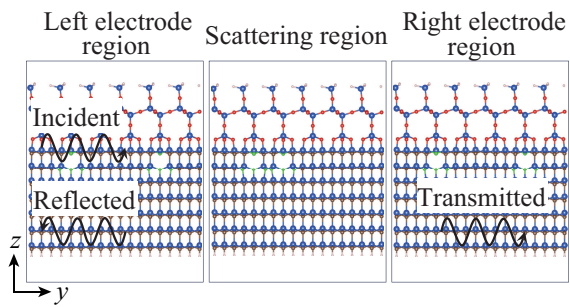


FIG. 3. Computational models for scattering-property calculation. Blue, red, brown, green, and gray balls are Si, O, C, N, and H atoms, respectively.

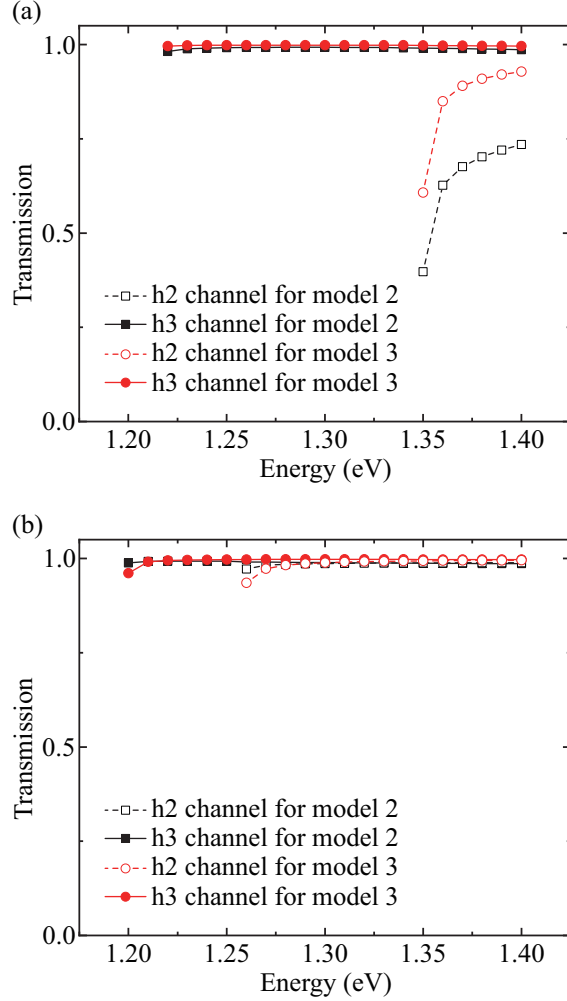


FIG. 4. Transmissions of (a) h- and (b) k-type interfaces at h2 and h3 channels. Energy is measured from the Fermi level.

The computational models for the electronic structure calculation are shown in Figs. 1(a) – 1(g). The RSPACE code^{21–23} which uses the real-space finite-difference approach^{24,25} for the DFT²⁰ is employed. According to scanning transmission electron microscopy images,²⁶ most of the SiO₂ in the SiC(0001)/SiO₂ interface is amorphous. However, it is not straightforward to characterize the interface atomic structure. The crystalline interface atomic structures that can exist locally at the SiC(0001)/SiO₂ interface proposed in our previous study²⁶ are employed. Our model contains a crystalline substrate with seven SiC bilayers (17.5 Å thick) connected without any coordination defects to a crystalline SiO₂ with a thickness of 8.2 Å. In a 4H-SiC bulk, SiC bilayers are stacked on the quasi-cubic (k) and hexagonal (h) sites alternately along the [0001] direction. We refer to the interface where the Si atoms in the topmost SiC bilayer are on the k (h) site as the k (h)-type

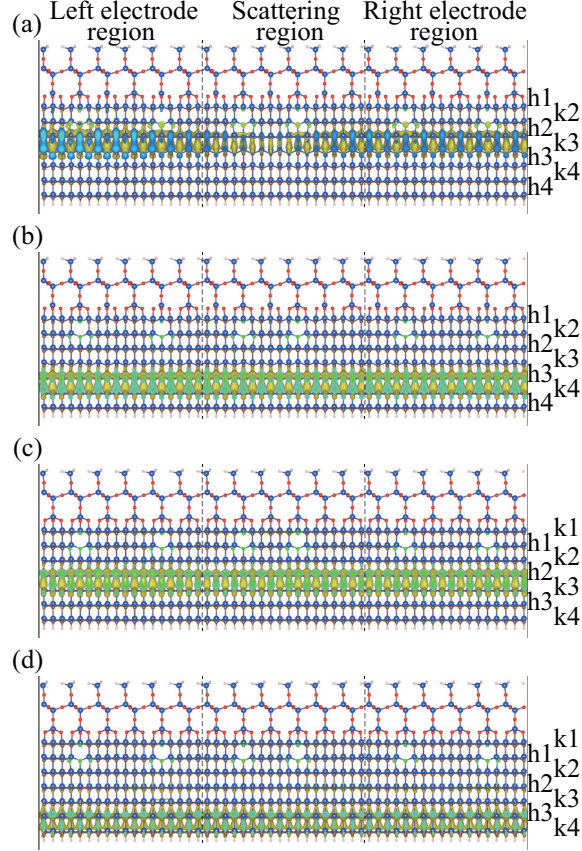


FIG. 5. Electron density distribution of scattering wavefunctions for (a) h2 channel at h-type interface, (b) h3 channel at h-type interface, (c) h2 channel at k-type interface, and (d) h3 channel at k-type interface for incident electrons with energy of $\varepsilon_F + 1.38$ eV. Blue, red, brown, green, and gray balls are Si, O, C, N, and H atoms, respectively.

interface. The electronic structures of the k-type interfaces are different from those of the h-type interfaces.¹⁶ Although it remains to be clarified whether the inserted N atoms exist on the SiO₂ or SiC side of the interface, we assume that the N atoms accumulate on the SiC side and the nitrated layers are formed at the interface on the basis of the possibility proposed in the previous experimental studies.^{19,27–30} For the nitrated region, we adopt the models proposed in our previous study, where a Si atom is removed and C atoms with dangling bonds (DBs) are replaced by N atoms.³¹ This structure has been proposed by Shirasawa *et al.*^{29,30} using low-energy electron diffraction analysis and a couple of N atoms accumulate near the Si vacancy to terminate DBs of Si atom in this structure. When all the possible sites of the interface are replaced by the nitrated regions, the areal N atom density is 1.22×10^{15} atom/cm², which is three times higher than the experimental value.¹⁹ We employ the interface models in which one third of the possible sites are replaced by the

nitrided regions. Hereafter, the nitrided layer with the high (low) areal N atom density is referred to as the fully (partially) nitrided layer. Three types of interface model are prepared as shown in Figs. 1(d) – 1(f) according to the distribution of the nitrided regions. The DBs at the top surface of the SiO₂ and the bottom surface of the SiC substrate are terminated by H atoms. The grid spacing in real space is taken to be $0.18 \times 0.19 \times 0.18 \text{ \AA}^3$. The exchange-correlation interaction is treated within the local density approximation of DFT.³² For electronic structure calculations, the periodic boundary condition is imposed on all the directions. The supercell size is $5.33 \times 27.72 \times 40.44 \text{ \AA}^3$. Integration over the Brillouin zone is performed using a $6 \times 2 \times 1$ k-point grid including Γ point. The projector augmented wave method³³ is adopted to describe the electron-ion interaction. We implement structural optimization until all the force components decrease to below 0.05 eV/\AA , while the atomic coordinates of the SiC bilayer in the bottom layer and the H atoms terminating DBs are fixed during the structural optimization.

The accumulation of the charges of CBE states is investigated using the partial charges,¹⁸ in which the wavefunctions of the CBE states of the interface are projected on those of the thin-film models as

$$\rho_{PC} = \sum_{i,k} |\langle \psi_{i,k} | \phi_k \rangle|^2 \theta(\epsilon_{i,k} - \epsilon_F) \theta(\epsilon_{max} - \epsilon_{i,k}) \Delta_k, \quad (1)$$

where ϵ_F is the Fermi level, θ is the Heaviside function, and ϕ_k is the wavefunction of the CBE states using the thin-film models. $\epsilon_{max}(=\epsilon_F + 1.65 \text{ eV})$, which is the maximum energy of the energy window, is chosen so that the energy window contains floating states inside the SiC substrate. The thin-film models for obtaining partial charges are illustrated in Fig. 1(f). SiC bilayers are stacked with hkh ordering in the thin-film model because it is reported that the CBE states lie below the Si atom of the h site in the (0001) face.¹⁶ The DBs on both sides of the surface are terminated by H atoms. Although the termination of surface atoms may change the magnitude of the partial charges, our conclusion is not affected because the same termination is employed for all thin-film models of SiC. The supercell size is chosen to be $5.33 \times 27.72 \times 40.44 \text{ \AA}^3$, which is the same as those for the interface.

The partial charges of the interface with the nitrided regions are shown in Fig. 2. The values of the partial charge at the partially nitrided layers are insensitive to the distribution of the nitrided regions while they are smaller than those without the nitrided regions. The CBE states at the interface are removed even when the areal N atom density is reduced and the Coulomb interaction of the O atoms in the SiO₂ is screened by the partially nitrided layer. However, the partial charge

at the partially nitrated layer is larger than that at the fully nitrated layer, indicating that the effect of NO annealing may be limited.

We then investigate the carrier scattering property at the interface because the Kohn-Sham effective potential is disturbed by the nonuniformly inserted nitrated regions. Figure 3 shows the computational models for the carrier-scattering property calculation. The computational models are divided into three parts; left electrode, scattering, and right electrode regions and the Kohn-Sham effective potential of these regions is obtained by repeating that of the primitive unit cell in the y direction. The left and right electrodes are set to be model 1 in Fig. 1(d) where the nitrated regions are inserted at equal intervals and the scattering region is set to be model 2 in Fig. 1(e) or model 3 in Fig. 1(f) so that the intervals of the nitrated regions are disordered. The electron-ion interaction is described by the norm-conserving pseudopotentials proposed by Troullier and Martins.³⁴⁻³⁶ The scattering wavefunctions for the incident electrons from the left electrode to the right electrode are evaluated by the overbridging-boundary matching method.³⁷⁻³⁹

The transmissions of the h- and k-type interfaces are shown in Fig. 4. The charge density distribution of the scattering wavefunction for the h-type interface is plotted in Fig. 5. The transmission channels can be categorized into two types from the charge density distribution of the scattering wavefunctions. The channels where the electrons accumulate near the interface and inside the substrate are referred to as the h2 and h3 channels, respectively. It is found that the transmissions of the h2 channel are lower than those of the h3 channel. In addition, the electrons flowing inside the h2 channel of the h-type interface are more significantly scattered than those flowing inside the h2 channel of the k-type interface because the h2 channel of the h-type interface is closer to the nitrated layer than that of the k-type interface. In our previous study, we have reported that the O interstitials which appear during thermal oxidation significantly scatter electrons as well as the typical interface defects at the SiC/SiO₂ interface.⁴⁰ The present results for the partially nitrated layer are consistent with the conclusion of our previous study on O interstitials. In addition, the Hall mobility remains low even after NO annealing as reported by Hatakeyama *et al.*¹⁴ and the N atoms incorporated into the SiC side of the interface do not contribute to improve Hall mobility as reported by Hosoi *et al.*⁴¹ The significant carrier scattering at the partially nitrated layer agrees with their experimental results. In the nitrated region proposed by low-energy electron diffraction analysis,^{29,30} there are a couple of N atoms in the vicinity of the Si vacancy to passivate the DBs and the potentials of the partially nitrated layer, where the areal N atom density is low, are fluctuated. Concerning the carrier scattering property, the present results suggest that the fully nitrated

layer with the high areal N atom density is better than the partially nitrated layer.

In summary, the effect of the nitrated layer introduced by NO annealing on the electronic structure and carrier scattering property of the SiC(0001)/SiO₂ interface has been investigated by density functional theory calculation. The areal N atom density was reduced from our previous study to replicate the interface of practical devices after NO annealing. It is found that the unfavorable effect of the O atoms in the SiO₂ can be screened by the nitrated layer even when the areal N atom density is reduced. However, the conducting electrons flowing just beneath the partially nitrated layer are scattered in the case of the h-type interface. On the other hand, in the case of the k-type interface, the transmission of the conducting electrons is unity because the layer where the electrons flow is separated from the nitrated layer. The fluctuation of the potential due to the low areal N atom density reduces the transmission and the scattering mechanism is same to that at the SiC(0001)/SiO₂ interface after thermal oxidation,⁴⁰ suggesting that the fully nitrated layer is better than the partially nitrated layer from the view point of carrier scattering property.

This work was partially financially supported by MEXT as part of the JSPS KAKENHI (24H01196, 24K01346). The numerical calculations were carried out using the computer facilities of the Institute for Solid State Physics at The University of Tokyo, the Center for Computational Sciences at University of Tsukuba, and the supercomputer Fugaku provided by the RIKEN Center for Computational Science (Project ID: hp230175, hp240178, hp250193).

DATA AVAILABILITY

The data that support the findings of this study are available from the corresponding author upon reasonable request.

REFERENCES

- ¹H. Okumura, *Jpn. J. Appl. Phys.* **45**, 7565 (2006).
- ²T. Kimoto, *Jpn. J. Appl. Phys.* **54**, 040103 (2015).
- ³K. Hamada, S. Hino, N. Miura, H. Watanabe, S. Nakata, E. Suekawa, Y. Ebiike, M. Imaizumi, I. Umezaki, and S. Yamakawa, *Jpn. J. Appl. Phys.* **54**, 04DP07 (2015).
- ⁴T. Kimoto and H. Watanabe, *Appl. Phys. Express* **13**, 120101 (2020).
- ⁵V. V. Afanasev, M. Bassler, G. Pensl, and M. Schulz, *Phys. Status Solidi A* **162**, 321 (1997).

- ⁶N. S. Saks and A. K. Agarwal, Appl. Phys. Lett. **77**, 3281 (2000).
- ⁷T. Hatakeyama, T. Watanabe, M. Kushibe, K. Kojima, S. Imai, T. Suzuki, T. Shinohe, T. Tanaka, and K. Arai, Mater. Sci. Forum **433**, 443 (2003).
- ⁸G. Chung, C. Tin, J. Williams, K. McDonald, R. Chanana, R. Weller, S. Pantelides, L. Feldman, O. Holland, M. Das, and J. Palmour, IEEE Electron Device Lett. **22**, 176 (2001).
- ⁹H.-f. Li, S. Dimitrijević, H. B. Harrison, and D. Sweatman, Appl. Phys. Lett. **70**, 2028 (1997).
- ¹⁰S. Harada, R. Kosugi, J. Senzaki, W.-J. Cho, K. Fukuda, K. Arai, and S. Suzuki, J. Appl. Phys. **91**, 1568 (2002).
- ¹¹Y. Nanen, M. Kato, J. Suda, and T. Kimoto, IEEE Trans. Electron Devices **60**, 1260 (2013).
- ¹²S. Nakazawa, T. Okuda, J. Suda, T. Nakamura, and T. Kimoto, IEEE Trans. Electron Devices **62**, 309 (2015).
- ¹³T. Hatakeyama, Y. Kiuchi, M. Sometani, S. Harada, D. Okamoto, H. Yano, Y. Yonezawa, and H. Okumura, Appl. Phys. Express **10**, 046601 (2017).
- ¹⁴T. Hatakeyama, T. Masuda, M. Sometani, S. Harada, D. Okamoto, H. Yano, Y. Yonezawa, and H. Okumura, Appl. Phys. Express **12**, 021003 (2019).
- ¹⁵Y.-i. Matsushita, S. Furuya, and A. Oshiyama, Phys. Rev. Lett. **108**, 246404 (2012).
- ¹⁶C. J. Kirkham and T. Ono, J. Phys. Soc. Jpn. **85**, 024701 (2016).
- ¹⁷N. Kuroda, K. Shibahara, W. Yoo, S. Nishino, and H. Matsunami, in *Extended Abstracts of the 19th Conference on Solid State Devices and Materials* (1987) p. 227.
- ¹⁸M. Uemoto, N. Funaki, K. Yokota, T. Hosoi, and T. Ono, Appl. Phys. Express **17**, 011009 (2024).
- ¹⁹K. Hamada, A. Mikami, H. Naruoka, and K. Yamabe, e-J. Surf. Sci. Nanotechnol. **15**, 109 (2017).
- ²⁰P. Hohenberg and W. Kohn, Phys. Rev. **136**, B864 (1964).
- ²¹T. Ono and K. Hirose, Phys. Rev. Lett. **82**, 5016 (1999).
- ²²K. Hirose, T. Ono, Y. Fujimoto, and S. Tsukamoto, *First-Principles Calculations in Real-Space Formalism – Electronic Configurations and Transport Properties of Nanostructures* (Imperial College Press, London, 2005).
- ²³T. Ono, M. Heide, N. Atodiresei, P. Baumeister, S. Tsukamoto, and S. Blügel, Phys. Rev. B **82**, 205115 (2010).
- ²⁴J. R. Chelikowsky, N. Troullier, and Y. Saad, Phys. Rev. Lett. **72**, 1240 (1994).
- ²⁵J. R. Chelikowsky, N. Troullier, K. Wu, and Y. Saad, Phys. Rev. B **50**, 11355 (1994).

- ²⁶T. Ono, C. J. Kirkham, S. Saito, and Y. Oshima, *Phys. Rev. B* **96**, 115311 (2017).
- ²⁷S. Dhar, L. C. Feldman, K.-C. Chang, Y. Cao, L. M. Porter, J. Bentley, and J. R. Williams, *J. Appl. Phys.* **97**, 074902 (2005).
- ²⁸K. Moges, M. Sometani, T. Hosoi, T. Shimura, S. Harada, and H. Watanabe, *Appl. Phys. Express* **11**, 101303 (2018).
- ²⁹T. Shirasawa, K. Hayashi, S. Mizuno, S. Tanaka, K. Nakatsuji, F. Komori, and H. Tochiwara, *Phys. Rev. Lett.* **98**, 136105 (2007).
- ³⁰T. Shirasawa, K. Hayashi, H. Yoshida, S. Mizuno, S. Tanaka, T. Muro, Y. Tamenori, Y. Harada, T. Tokushima, Y. Horikawa, E. Kobayashi, T. Kinoshita, S. Shin, T. Takahashi, Y. Ando, K. Akagi, S. Tsuneyuki, and H. Tochiwara, *Phys. Rev. B* **79**, 241301 (2009).
- ³¹M. Uemoto, N. Komatsu, Y. Egami, and T. Ono, *J. Phys. Soc. Jpn.* **90**, 124713 (2021).
- ³²S. H. Vosko, L. Wilk, and M. Nusair, *Can. J. Phys.* **58**, 1200 (1980).
- ³³P. E. Blöchl, *Phys. Rev. B* **50**, 17953 (1994).
- ³⁴K. Kobayashi, *Comput. Mater. Sci.* **14**, 72 (1999).
- ³⁵N. Troullier and J. L. Martins, *Phys. Rev. B* **43**, 1993 (1991).
- ³⁶L. Kleinman and D. M. Bylander, *Phys. Rev. Lett.* **48**, 1425 (1982).
- ³⁷Y. Fujimoto and K. Hirose, *Phys. Rev. B* **67**, 195315 (2003).
- ³⁸T. Ono and K. Hirose, *Phys. Rev. B* **70**, 033403 (2004).
- ³⁹S. Tsukamoto, T. Ono, S. Iwase, and S. Blügel, *Phys. Rev. B* **98**, 195422 (2018).
- ⁴⁰S. Iwase, C. J. Kirkham, and T. Ono, *Phys. Rev. B* **95**, 041302 (2017).
- ⁴¹T. Hosoi, M. Ohsako, K. Moges, K. Ito, T. Kimoto, M. Sometani, M. Okamoto, A. Yoshigoe, T. Shimura, and H. Watanabe, *Appl. Phys. Express* **15**, 061003 (2022).